

## A Statistical Generalization of the Transformed Eulerian-Mean Circulation for an Arbitrary Vertical Coordinate System

OLIVIER PAULUIS, TIFFANY SHAW,\* AND FRÉDÉRIC LALIBERTÉ

*Courant Institute of Mathematical Sciences, New York University, New York, New York*

(Manuscript received 22 October 2010, in final form 1 February 2011)

### ABSTRACT

A new method is derived for approximating the mean meridional circulation in an arbitrary vertical coordinate system using only the time-mean and zonally averaged meridional velocity, meridional eddy transport, and eddy variance. The method is called the statistical transformed Eulerian mean (STEM) and can be viewed as a generalization of the transformed Eulerian mean (TEM) formulation. It is shown that the TEM circulation can be obtained from the STEM circulation in the limit of small eddy variance. The main advantage of the STEM formulation is that it can be applied to nonmonotonic coordinate systems such as the equivalent potential temperature. In contrast, the TEM formulation can only be applied to stratified variables. Reanalysis data are used to compare the STEM circulation to an explicit calculation of the mean meridional circulation on dry and moist isentropic surfaces based on daily data. It is shown that the STEM formulation accurately captures all the key features of the circulation. The error in the streamfunction is less than 10%.

The STEM formulation is subsequently used to analyze the circulation induced by latent heat transport and to understand the processes responsible for setting the effective stratification in the troposphere. The eddy sensible heat transport dominates in the midlatitudes and in the winter hemisphere, while the eddy latent heat transport dominates in the subtropical regions and in the summer hemisphere. For the dry isentropic circulation, the approximate effective stratification is dominated by the vertical stratification, whereas for the moist isentropic circulation it is dominated by the eddy variance contribution. The importance of the eddy variance in setting the stratification is in agreement with previous work.

### 1. Introduction

The global atmospheric circulation is characterized by a vast range of length scales which span a few meters for isotropic turbulence inside a cloud to thousands of kilometers for the tropical Hadley circulation. The turbulent nature of the flow leads to a particular challenge when trying to describe the global circulation. A natural approach would be to compute a time- and zonally averaged circulation. However, the resulting circulation depends on the choice of vertical coordinate. A classical example of this dependence is the difference between the

Eulerian-mean circulation, which is obtained by averaging the meridional mass transport on surfaces of constant pressure or geopotential height, and the dry isentropic circulation, which is obtained by averaging on surfaces of constant potential temperature. The Eulerian-mean circulation exhibits a three-cell structure in each hemisphere with the Hadley cell in the tropics, the Ferrel cell in the midlatitudes, and the polar cell at high latitudes (see Peixoto and Oort 1992, among others). In contrast, the dry isentropic circulation has a single direct equator-to-pole overturning cell with high potential temperature air flowing toward the poles and lower potential temperature air flowing toward the equatorial regions (see, e.g., Townsend and Johnson 1985; Johnson 1989; Jukes et al. 1994; Held and Schneider 1999). Recently, Czaja and Marshall (2006) and Pauluis et al. (2008, 2010) showed that the moist isentropic circulation, which is obtained by averaging the meridional circulation on surfaces of constant equivalent potential temperature, also exhibits a single equator-to-pole overturning cell. However, it has a significantly larger mass transport

---

\* Current affiliation: Lamont-Doherty Earth Observatory, and Department of Applied Physics and Applied Mathematics, Columbia University, New York, New York.

---

Corresponding author address: Olivier Pauluis, Courant Institute of Mathematical Sciences, New York University, Warren Weaver Hall, 251 Mercer St., New York, NY 10012-1185.  
E-mail: pauluis@cims.nyu.edu

than the dry isentropic circulation. On a qualitative level, the difference between the dry and moist circulations can be explained by the poleward transport of sensible and latent heat by midlatitude eddies. Other choices of averaging surfaces have been proposed including potential vorticity and humidity (Jukes 2001; Döös and Nilsson 2011), which provide insight into different aspects of the mean meridional circulation. This raises the question of how the mean meridional circulations obtained by different averaging procedures can be related to one another.

The difference between the Eulerian-mean and dry isentropic circulations can be understood, in part, using the transformed Eulerian mean (TEM) formulation (Andrews and McIntyre 1976; Edmon et al. 1980; Andrews et al. 1987; McIntosh and McDougall 1996; Jukes 2001). In the TEM formulation, the residual or total circulation is the sum of an Eulerian-mean circulation and an eddy-induced circulation. The Eulerian-mean contribution is exactly the circulation averaged on pressure surfaces as discussed above, while the eddy-induced contribution is proportional to the meridional energy transport by eddies weighted by the vertical stratification of potential temperature. The eddy-induced circulation corresponds to a direct overturning cell and dominates in midlatitudes. Andrews and McIntyre (1978) have shown formally that the eddy-induced circulation in the TEM corresponds to a wave-induced Stoke drift in the small-amplitude limit. The TEM residual circulation exhibits the single-cell structure of the dry isentropic circulation.

Held and Schneider (1999) have shown that although the TEM and dry isentropic circulations are qualitatively similar, there are notable differences. In particular, the TEM circulation does not close at the surface. Instead it exhibits an infinite return flow because the meridional eddy heat transport only vanishes in a very thin surface layer, which is unresolved in global datasets. Another important limitation of the TEM formulation is that it requires the atmosphere to be stratified with respect to potential temperature. This means that the TEM formulation cannot be applied in regions where the stratification vanishes (e.g., in the boundary layer). Several authors (Held and Schneider 1999; Plumb and Ferrari 2005) have proposed different methods to circumvent this problem at the cost of losing some of the original formalism of the TEM. In the boundary layer, Held and Schneider (1999) replace the vertical stratification by the meridional stratification and the meridional eddy flux by the vertical flux. Plumb and Ferrari (2005) generalized their method by decomposing the eddy fluxes into adiabatic (along isentropic) and diabatic (cross isentropic) contributions. While their method can be applied in regions of vanishing vertical stratification (e.g., in the oceanic mixed layer), the resulting residual

circulation does not account for the meridional eddy transport in such regions. Jukes (2001) also generalized the TEM formulation so that it could be applied to an arbitrary variable instead of the potential temperature; however, the generalization still requires a monotonic variable in the vertical. Similarly, Stone and Salusti (1994) generalized the Eliassen–Palm flux and TEM residual circulation to include eddy-induced water vapor transport, but their formulation can only be used in regions where the equivalent potential temperature is monotonic. When considering the moist circulation one must confront the fact that the equivalent potential temperature often exhibits a local minimum in the lower troposphere where the meridional eddy transport of water vapor is large. This has so far precluded the application of the TEM formulation and its generalizations to the moist circulation.

The purpose of this paper is to further generalize the TEM formulation so that it can be applied when the state variable is unstratified. In doing so we aim to gain new insight into the global atmospheric circulation and the dependence of its description on the choice of vertical coordinate. Section 2 outlines a generalization of the TEM formulation based on a statistical interpretation of the eddy transport, called the statistical transformed Eulerian mean (STEM), which approximates the meridional circulation averaged in an arbitrary vertical coordinate using the Eulerian-mean circulation and quadratic eddy statistics. In section 3, the STEM formulation is applied to reanalysis data to reconstruct the dry and moist isentropic circulations and the results are compared to exact calculations of the circulations. The STEM circulation is shown to accurately capture all the key features of the dry and moist isentropic circulations. In section 4, we show that the TEM formulation represents a special limit of the STEM formulation. Section 5 explores the implications of the STEM formulation for the dry and moist stratifications in midlatitudes. In section 6, we summarize our results and discuss possible extensions of the STEM formulation.

## 2. Statistical transformed Eulerian mean

We begin by assuming that we are given the time-averaged, zonal-mean atmospheric state and quadratic eddy statistics of  $v$  and an arbitrary state variable  $\zeta$  in an Eulerian frame with pressure or geopotential height as the vertical coordinate. In particular, we assume that we are given the time and zonal average of  $\bar{\zeta}$  and  $\bar{v}$ , where the overbar denotes the time and zonal average, as well as the eddy meridional transport and eddy variance of the state variable (i.e.,  $\overline{\zeta'v'}$  and  $\overline{\zeta'^2}$ , where the prime denotes the deviation from a zonal average on pressure surfaces). The state

variable can be the potential temperature  $\theta$ , the equivalent potential temperature  $\theta_e$ , the specific humidity  $q$ , etc. Using the mean and eddy information, we would like to obtain the meridional circulation averaged on iso- $\zeta$  surfaces.

We define a joint distribution for the meridional mass transport  $m(p, \zeta, \phi) dp d\zeta$  as the time- and zonally averaged meridional mass transport between pressure values  $p$  and  $p + dp$  and between state variable values  $\zeta$  and  $\zeta + d\zeta$  at a latitude  $\phi$ . Using this notation, the meridional mass transport on pressure surfaces  $M_p(p, \phi)$  is given by

$$M_p(p, \phi) = \int_0^\infty m(p, \tilde{\zeta}, \phi) d\tilde{\zeta} = \frac{2\pi a \cos\phi}{g} \bar{v}(p, \phi), \quad (1)$$

where  $a$  is the radius of the earth and  $g$  is the gravitational acceleration. Note that we assume that the meridional velocity, and hence the meridional mass transport, vanishes when the pressure is greater than the surface pressure. The meridional mass transport on iso- $\zeta$  surfaces is given by

$$M_\zeta(\zeta, \phi) = \int_{-\infty}^\infty m(\tilde{p}, \zeta, \phi) d\tilde{p}. \quad (2)$$

The mass transports (1) and (2) can be converted into streamfunctions upon integrating; that is,

$$\Psi_p(p, \phi) = \int_0^p M_p(\tilde{p}, \phi) d\tilde{p} = \int_0^p \int_{-\infty}^\infty m(\tilde{p}, \tilde{\zeta}, \phi) d\tilde{\zeta} d\tilde{p}, \quad (3a)$$

$$\Psi_\zeta(\zeta, \phi) = \int_{-\infty}^\zeta M_\zeta(\tilde{\zeta}, \phi) d\tilde{\zeta} = \int_{-\infty}^\zeta \int_0^\infty m(\tilde{p}, \tilde{\zeta}, \phi) d\tilde{p} d\tilde{\zeta}. \quad (3b)$$

This definition of the streamfunction  $\Psi_\zeta$  can be robustly applied to an arbitrary coordinate system  $\zeta$ , even one that does not vary monotonically with pressure. In such a case,  $\Psi_\zeta$  may include contributions from multiple pressure levels. One should thus be careful in interpreting the streamfunction as it may not correspond to a geometric overturning; rather, it captures mass transports associated with different (thermodynamic) properties. For example, Pauluis et al. (2008, 2010) showed that the enhanced mass transport on moist isentropes can be attributed to a combination of a poleward flow of high  $\theta$  air in the upper troposphere and a low-level poleward flow of warm moist air with a comparable value of  $\theta_e$ .

Our ability to calculate the iso- $\zeta$  circulation  $\Psi_\zeta$  from (3b) depends on whether  $m(p, \zeta, \phi)$  can be reconstructed with sufficient accuracy. A direct calculation of  $m(p, \zeta, \phi)$  is straightforward when given data with sufficient spatial and temporal resolution. However, here we assume that

we are only given monthly and zonally averaged data, which are commonly output from climate models and cannot be used to reconstruct the mass transport distribution directly. Thus, the mass transport distribution must be approximated in order to recover the iso- $\zeta$  circulation.

Under the assumption that we are given the mean atmospheric state and quadratic eddy statistics, the simplest approach is to assume that the eddy-induced fluctuations obey a Gaussian distribution. This Gaussian assumption is purely a kinematic one and relies on a statistical interpretation of the eddy transport. To emphasize this, we call the formulation, which is derived below, the STEM formulation. The Gaussian distribution requires knowledge of the mean values  $\bar{v}(p, \phi)$  and  $\bar{\zeta}(p, \phi)$ , the variances  $\overline{v'^2}(p, \phi)$  and  $\overline{\zeta'^2}(p, \phi)$ , and the covariance  $\overline{v'\zeta'}(p, \phi)$ . In appendix A, it is shown that under the Gaussian assumption the joint distribution of the meridional mass transport per unit  $\zeta$  and unit  $p$  can be decomposed as

$$m(p, \zeta, \phi) = m_{\text{mean}}(p, \zeta, \phi) + m_{\text{eddy}}(p, \zeta, \phi), \quad (4)$$

where  $m_{\text{mean}}$  and  $m_{\text{eddy}}$  are the Eulerian-mean and eddy components defined in (A6a) and (A6b) as

$$m_{\text{mean}}(p, \zeta, \phi) = \frac{2\pi a \cos\phi}{g} \frac{\bar{v}}{\sqrt{2\pi\zeta'^2}^{1/2}} \exp\left[-\frac{(\zeta - \bar{\zeta})^2}{2\zeta'^2}\right], \quad (5a)$$

$$m_{\text{eddy}}(p, \zeta, \phi) = \frac{2\pi a \cos\phi}{g} \frac{\overline{v'\zeta'}(\zeta - \bar{\zeta})}{\sqrt{2\pi\zeta'^2}^{3/2}} \exp\left[-\frac{(\zeta - \bar{\zeta})^2}{2\zeta'^2}\right]. \quad (5b)$$

The Eulerian-mean component of the meridional mass transport is obtained upon plugging (5a) into (2) and is equal to the convolution of the meridional mass transport with a Gaussian distribution with eddy variance  $\zeta'^2$ ; that is,

$$M_{\zeta, \text{mean}}(\zeta, \phi) = \int_0^\infty m_{\text{mean}}(\tilde{p}, \zeta, \phi) d\tilde{p} = \int_0^\infty \frac{2\pi a \cos\phi}{g} \frac{\bar{v}}{\sqrt{2\pi\zeta'^2}^{1/2}} \exp\left[-\frac{(\zeta - \bar{\zeta})^2}{2\zeta'^2}\right] d\tilde{p}. \quad (6)$$

This convolution has two direct effects. First, it will broaden the mass transport by redistributing it over a broader range of iso- $\zeta$  surfaces when the eddy variance is large. It also allows for mass transport on ‘‘underground’’ iso- $\zeta$  surfaces with  $\zeta < \tilde{\zeta}(p_{\text{surf}}, \phi)$ , where  $p_{\text{surf}}$  is the time and zonal mean surface pressure. Second, when  $\tilde{\zeta}(p, \phi)$  is nonmonotonic in  $p$ , (5a) automatically folds the circulation by summing the contribution of all isobaric surfaces.

The eddy component of the meridional mass transport is given by the convolution of the eddy transport and the derivative of the Gaussian distribution:

$$\begin{aligned}
 M_{\zeta,\text{eddy}}(\zeta, \phi) &= \int_0^\infty m_{\text{eddy}}(\tilde{p}, \zeta, \phi) d\tilde{p} \\
 &= \int_0^\infty \frac{2\pi a \cos\phi}{g} \frac{v'\zeta'(\zeta - \bar{\zeta})}{\sqrt{2\pi\zeta'^2}^{3/2}} \exp\left[-\frac{(\zeta - \bar{\zeta})^2}{2\zeta'^2}\right] d\tilde{p}.
 \end{aligned}
 \tag{7}$$

The eddy component of the meridional mass transport is decomposed into two opposite flows that take place at values of  $\zeta$  that are above and below the mean value  $\bar{\zeta}(p, \phi)$ .

The STEM streamfunction  $\Psi_{\zeta,\text{STEM}}$  can also be divided into Eulerian-mean and eddy contributions; for example,

$$\Psi_{\zeta,\text{STEM}}(\zeta, \phi) = \Psi_{\zeta,\text{mean}}(\zeta, \phi) + \Psi_{\zeta,\text{eddy}}(\zeta, \phi), \tag{8}$$

where the two contributions are given by

$$\Psi_{\zeta,\text{mean}}(\zeta, \phi) = \int_{-\infty}^{\zeta} \int_0^\infty m_{\text{mean}}(\tilde{p}, \tilde{\zeta}, \phi) d\tilde{p} d\tilde{\zeta} \quad \text{and} \tag{9a}$$

$$\Psi_{\zeta,\text{eddy}}(\zeta, \phi) = \int_{-\infty}^{\zeta} \int_0^\infty m_{\text{eddy}}(\tilde{p}, \tilde{\zeta}, \phi) d\tilde{p} d\tilde{\zeta}. \tag{9b}$$

Note that in contrast to the TEM formulation, which retains the pressure vertical coordinate after the transformation, the STEM streamfunction is obtained on iso- $\zeta$  surfaces. The relationship between the STEM and TEM formulations is discussed in detail in section 4.

### 3. Reconstructing the isentropic circulations using the STEM formulation

As described in the previous section, the STEM circulation can be calculated from monthly and zonally averaged data. These data can come from reanalysis products or climate models. Here we use the National Centers for Environmental Prediction (NCEP) reanalysis data (Kalnay et al. 1996) from 1979 to 2009 to calculate the STEM circulation for  $\zeta = \theta$  and  $\zeta = \theta_e$ . In particular, we calculate  $\bar{v}$ ,  $\bar{\theta}$ ,  $v'\theta'$ ,  $\theta'^2$ ,  $\overline{\theta_e}$ ,  $v'\theta'_e$ , and  $\theta_e'^2$  (where the overbar represents a monthly and zonal average and the prime indicates a deviation from the zonal average only) on pressure surfaces using the NCEP data, and then apply the STEM procedure to reconstruct the circulations on dry and moist isentropes. The STEM circulations are then compared to exact calculations of the dry and moist isentropic circulations to assess the accuracy

of the STEM formulation. The exact isentropic circulations are computed using daily three-dimensional NCEP data following Pauluis et al. (2010):

$$\Psi_\theta(\theta, \phi) = \frac{a \cos\phi}{T} \int_0^T \int_0^{2\pi} \int_0^{p_{\text{surf}}} vH[\theta - \tilde{\theta}(\tilde{\lambda}, \phi, \tilde{p}, \tilde{t})] \frac{d\tilde{p}}{g} d\tilde{\lambda} d\tilde{t}, \tag{10a}$$

$$\Psi_{\theta_e}(\theta_e, \phi) = \frac{a \cos\phi}{T} \int_0^T \int_0^{2\pi} \int_0^{p_{\text{surf}}} vH[\theta_e - \tilde{\theta}_e(\tilde{\lambda}, \phi, \tilde{p}, \tilde{t})] \frac{d\tilde{p}}{g} d\tilde{\lambda} d\tilde{t}, \tag{10b}$$

where  $T$  is the time period over which the circulation is averaged (one month in this case),  $\lambda$  is the longitude, and  $H$  is the Heaviside function.

Figures 1 and 2 show the STEM circulation for  $\zeta = \theta$  and the exact calculation of the dry isentropic circulation during December–February (DJF) and June–August (JJA), respectively. In both figures the top left panel shows the Eulerian-mean component of the STEM circulation  $\Psi_{\theta,\text{mean}}$ , the top right panel shows the eddy component of the STEM circulation  $\Psi_{\theta,\text{eddy}}$ , the bottom left panel is the STEM residual circulation  $\Psi_{\theta,\text{STEM}}$ , and the bottom right panel is the dry isentropic circulation  $\Psi_\theta$  obtained from the exact calculation.

The Eulerian-mean component of the STEM circulation  $\Psi_{\theta,\text{mean}}$  is dominated by the cross-equatorial Hadley cell during both DJA and JJA. The summer hemisphere Hadley cell is significantly weaker than the cross-equatorial cell, and during JJA it is below the contour interval. The Ferrel cells are also evident in the Eulerian-mean component in midlatitudes. During DJF there is a Ferrel cell in both hemispheres; however, the Ferrel cell in the summer hemisphere is particularly weak during JJA (it is below the contour interval). The eddy component of the STEM circulation  $\Psi_{\theta,\text{eddy}}$  involves a direct circulation in midlatitudes. During DJF there is an eddy-induced circulation in both hemispheres, but during JJA the circulation is very weak in the summer hemisphere. The Eulerian-mean and eddy components of the STEM circulation barely overlap in the winter hemisphere during both seasons.

The STEM residual circulation exhibits a single equator-to-pole overturning cell in both hemispheres during DJF similar to the exact isentropic circulation. However, during JJA there is only a single cell in the winter hemisphere; the circulation is very weak in the summer hemisphere. The STEM residual circulation does a reasonable job of reproducing the exact dry isentropic circulation (cf. the bottom panels in Figs. 1 and 2). Because the eddy statistics in the STEM formulation are approximated by a Gaussian distribution, one should not

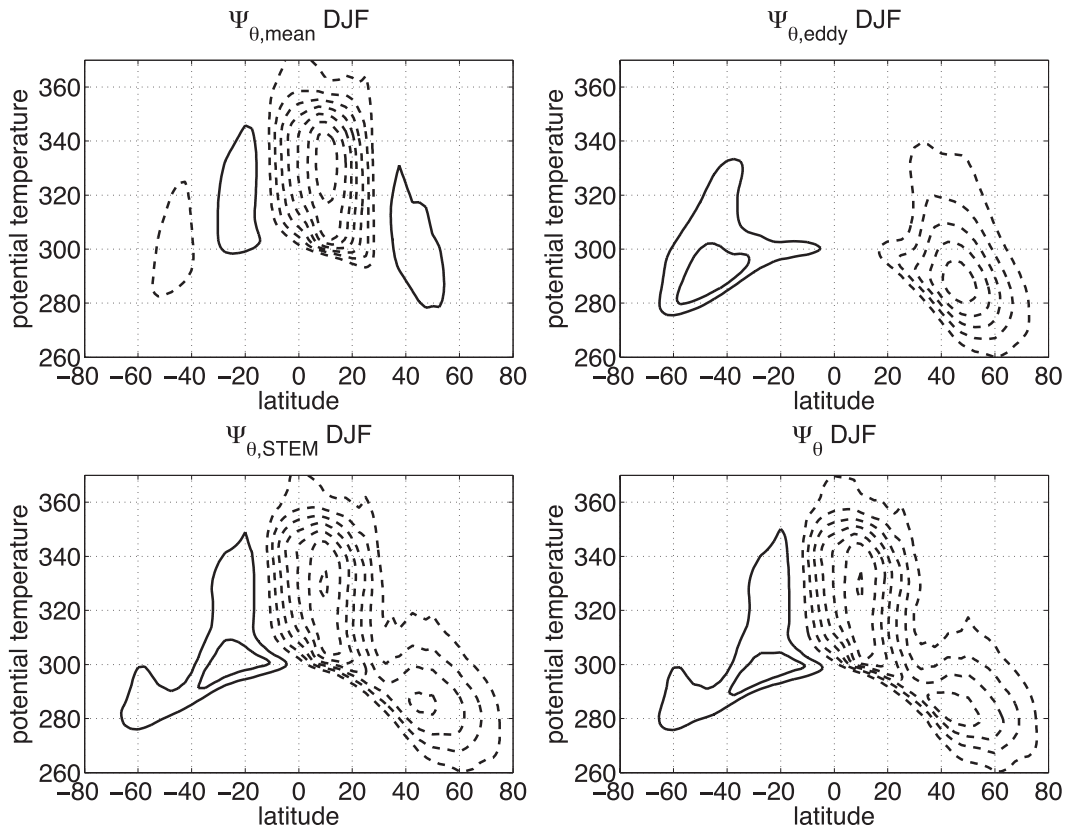


FIG. 1. Circulation on dry isentropes during DJF. (top left) Eulerian-mean circulation, (top right) eddy circulation, (bottom left) STEM residual circulation, and (bottom right) exact calculation of the isentropic circulation. Contour interval is  $2.0 \times 10^{10} \text{ kg s}^{-1}$  and negative contours representing clockwise motion are dashed.

expect perfect agreement. In general, the STEM circulations during DJF and JJA are a little weaker than the exact circulation in the lower tropical atmosphere and in the midlatitudes. The weaker circulation is partially compensated for by having the circulation extend through a deeper layer (in terms of potential temperature). The comparison between the two circulations is quantified below.

Figures 3 and 4 show the corresponding STEM circulation for  $\zeta = \theta_e$  and the exact calculation of the moist isentropic circulation during DJF and JJA, respectively. The Eulerian-mean component of the STEM circulation on moist isentropes  $\Psi_{\theta_e, \text{mean}}$  is qualitatively similar to the Eulerian-mean component on dry isentropes  $\Psi_{\theta, \text{mean}}$  (cf. Figs. 1 and 3, and Figs. 2 and 4). The moist Eulerian-mean circulation, however, is spread over a narrower range of isentropic surfaces than its dry counterpart because vertical variations in  $\theta_e$  are always smaller than vertical variations in  $\theta$ . In addition, there is some degree of cancellation between the lower and upper tropospheric flows, which occur at same value of  $\theta_e$ , resulting in a weaker net mass transport.

The eddy component of the STEM circulation on moist isentropes  $\Psi_{\theta_e, \text{eddy}}$  is much stronger than its dry counterpart. It includes both sensible and latent heat transports and is therefore larger than the eddy component on dry isentropes, which only accounts for sensible heat transport. A second notable difference is that the eddy circulation on moist isentropes extends farther into the equatorial regions than the circulation on dry isentropes. This extension is due to the extraction of water vapor from the deep tropics by baroclinic eddies. When the Eulerian-mean and eddy components of the circulation on moist isentropes are added together, the resulting STEM residual circulation exhibits a single equator-to-pole overturning cell similar to the dry isentropic circulation. However, the circulation on moist isentropes is significantly stronger in the midlatitudes and subtropics. Once again, the STEM circulation and the exact isentropic circulation are in very good agreement. As for the circulation on dry isentropes, the STEM residual circulation is slightly weaker and spread over a broader range of  $\theta_e$  values.

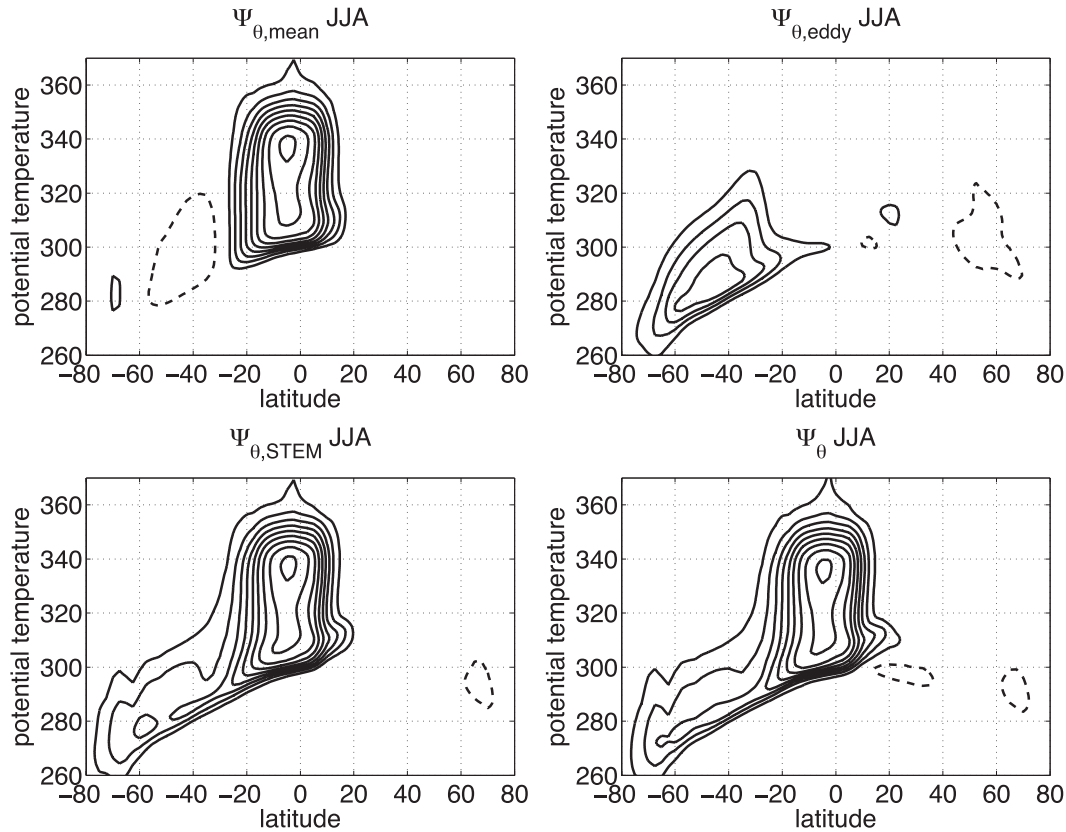


FIG. 2. As in Fig. 1, but for JJA.

The STEM formulation can be used to analyze the individual contributions of latent and sensible heat transport to the eddy component of the circulation on moist isentropes. In particular, the eddy transport of equivalent potential temperature can be decomposed as

$$\overline{v'\theta'_e} \approx \overline{v'\theta'} + \frac{L}{c_p} \overline{v'q'}, \quad (11)$$

where  $q$  is the water vapor concentration,  $L$  is the latent heat of vaporization of water, and  $c_p$  is the specific heat at constant pressure. This allows us to decompose the eddy component of the circulation into sensible and latent contributions

$$\Psi_{\theta_e, \text{eddy}}(\theta_e, \phi) = \Psi_{\theta_e, \text{SH}}(\theta_e, \phi) + \Psi_{\theta_e, \text{LH}}(\theta_e, \phi), \quad (12)$$

where the sensible and latent heat contributions are related to the potential temperature flux  $\overline{v'\theta'}$  and latent heat flux  $L\overline{v'q'}/c_p$ , respectively. The eddy component of the circulation on dry isentropes  $\Psi_{\theta, \text{eddy}}$  only includes sensible heat transport  $\overline{v'\theta'}$ .

Figure 5 shows the sensible and latent heat transport contributions to the eddy circulation on moist isentropes

during DJF (top) and JJA (bottom). The sensible heat transport contribution to the eddy circulation dominates in the mid- to high latitudes and in the winter hemisphere. Note that the sensible heat transport contribution to the moist and dry circulations are not equal because of the differences in the corresponding eddy variances  $\overline{\theta'^2}$  and  $\overline{\theta_e'^2}$ . The latent heat transport contribution is larger in the subtropics and in the summer hemisphere. The two heat transport contributions overlap significantly in midlatitudes—corresponding roughly to the regions of enhanced precipitation in the storm tracks—so that the eddy-induced circulation is larger than the individual sensible and latent heat transport contributions. The inclusion of latent heat transport both intensifies the eddy circulation and extends it toward the equator, reflecting the ability of baroclinic eddies to extract water vapor from the subtropics.

The STEM circulations for  $\zeta = \theta$  and  $\zeta = \theta_e$  can be quantitatively compared to the corresponding exact calculation of the isentropic circulations (10) by comparing the respective total isentropic mass transports. The total isentropic mass transport  $\Delta\Psi_\zeta$  is defined as the difference between the maximum and minimum of the streamfunction at a given latitude; that is,

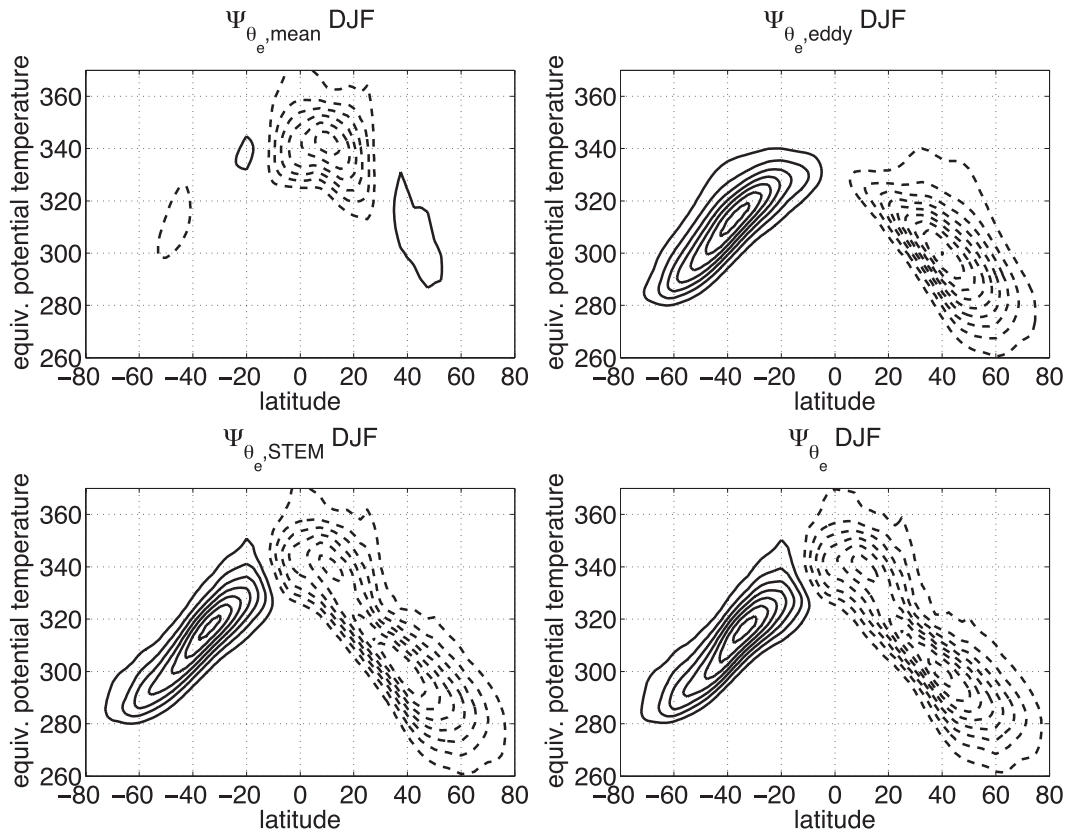


FIG. 3. As in Fig. 1, but for moist isentropes during DJF.

$$\Delta\Psi_{\zeta} = \max_{\zeta} \Psi_{\zeta} - \min_{\zeta} \Psi_{\zeta}. \quad (13)$$

Figure 6 shows the total isentropic mass transport for the exact circulation (solid line) and the STEM residual circulation (dashed line) during DJF (left) and JJA (right). In general, the STEM circulation underestimates the total mass transport. The maximum error is 10% for the dry isentropic circulation during DJF in the Northern Hemisphere. The maximum error for the moist circulation is less than 5%. This confirms that the STEM formulation is able to reproduce the qualitative and quantitative aspects of the dry and moist isentropic circulations using only monthly and zonally averaged data.

#### 4. Relationship between the STEM and TEM formulations

The STEM formulation derived in the previous section can be viewed as a generalization of the TEM formulation (Andrews and McIntyre 1976; Edmon et al. 1980; Andrews et al. 1987; Jukes 2001). In the TEM formulation, an eddy-induced circulation is added to the

Eulerian-mean circulation in pressure coordinates to produce the TEM residual circulation:

$$\Psi_{\text{TEM}}(p, \phi) = \Psi_{p,\text{mean}}(p, \phi) + \Psi_{p,\text{eddy}}(p, \phi), \quad (14)$$

where the mean contribution is identical to (3a). The eddy-induced circulation is proportional to the meridional eddy flux of potential temperature:

$$\Psi_{p,\text{eddy}}(p, \phi) = -\frac{2\pi a \cos\phi}{g} \left( \frac{\partial \bar{\theta}}{\partial p} \right)^{-1} \bar{v}'\theta'. \quad (15)$$

Because the eddy contribution is weighted by the vertical stratification, the TEM formulation can only be applied where the potential temperature is stratified in the vertical (i.e., outside the boundary layer). As discussed previously, the TEM formulation and its generalization by Held and Schneider (1999), Plumb and Ferrari (2005), and Jukes (2001) require a stratified state variable. They cannot be applied to the case of  $\zeta = \theta_e$ , which is our original motivation for developing the STEM formulation.

The TEM circulation can be obtained as a special solution of the STEM approximation. We consider the

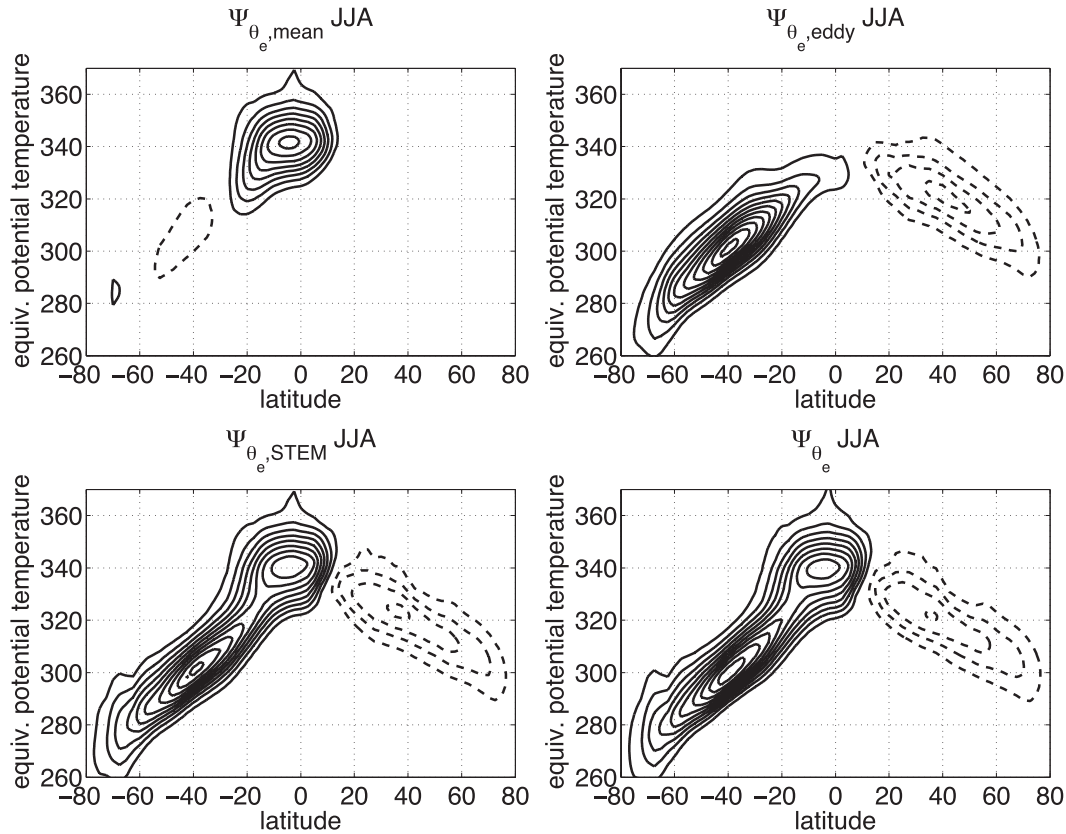


FIG. 4. As in Fig. 3, but for JJA.

STEM formulations in the limit where  $\bar{\zeta}(p)$  is strictly monotonic (and thus invertible), replace  $\bar{\zeta}^{\prime 2}$  with a constant, and compute the Eulerian-mean and eddy components of the streamfunction  $\Psi_{\theta,\text{mean}}$  and  $\Psi_{\theta,\text{eddy}}$ . In the limit of small eddy variance (shown in appendix B), the STEM streamfunctions converge to

$$\lim_{\zeta^{\prime 2} \rightarrow 0} \Psi_{\zeta,\text{mean}}[\bar{\zeta}(p), \phi] = \text{sgn}\left(\frac{\partial \bar{\zeta}}{\partial p}\right) \Psi_{p,\text{mean}}(p, \phi), \quad (16a)$$

$$\begin{aligned} \lim_{\zeta^{\prime 2} \rightarrow 0} \Psi_{\zeta,\text{eddy}}[\bar{\zeta}(p), \phi] &= -\frac{2\pi a \cos \phi}{g} \left| \frac{\partial \bar{\zeta}}{\partial p} \right|^{-1} v' \zeta'(p, \phi) \\ &= \text{sgn}\left(\frac{\partial \bar{\zeta}}{\partial p}\right) \Psi_{p,\text{eddy}}(p, \phi), \quad (16b) \end{aligned}$$

which are exactly the mean and eddy components of the TEM circulation [see (B3) and (B7)]. Thus, the TEM formulation corresponds to the small eddy variance limit of the STEM formulation. Note that the circulation changes sign if  $\bar{\zeta}$  decreases with pressure, which is a consequence of the choice of the limits of integration in the definition of the streamfunction [(3a) and (3b)].

Andrews and McIntyre (1978) showed that for a small-amplitude perturbation—that is, velocity  $v'$  and  $\zeta'$  perturbations  $O(\epsilon)$ —the TEM residual circulation induced by such a perturbation is  $O(\epsilon^2)$ . In such a case, the eddy variance is also  $O(\epsilon^2)$  and thus the small variance limit clearly applies. Equations (16a) and (16b) imply that in the small eddy variance limit the STEM circulation asymptotes to the leading-order TEM circulation.

The small variance limit, (16a) and (16b), provides insight into the differences between the TEM and STEM circulations for finite-amplitude perturbations. Indeed, (16b), which is derived assuming a small eddy variance, remains valid even for constant meridional transport  $\bar{v}' \zeta'$ ; that is, one can have a perturbation of magnitude  $\zeta^{\prime 2} \sim O(\epsilon^2)$  and have  $\bar{v}' \zeta' \sim O(1)$ . Figure 7 illustrates the dependence of the STEM circulation on the strength of the eddy variance. It shows the STEM residual circulation for  $\zeta = \theta$  during DJF and for constant  $\theta^{\prime 2} = 64, 16, 4,$  and  $1 \text{ K}^2$ . As the eddy variance is reduced, the equatorward flow becomes confined to a shallower and shallower underground layer (i.e., below the mean value of  $\theta$  at the surface). For small values of the eddy variance, the streamfunction exhibits a sharp transition from a finite value through zero in



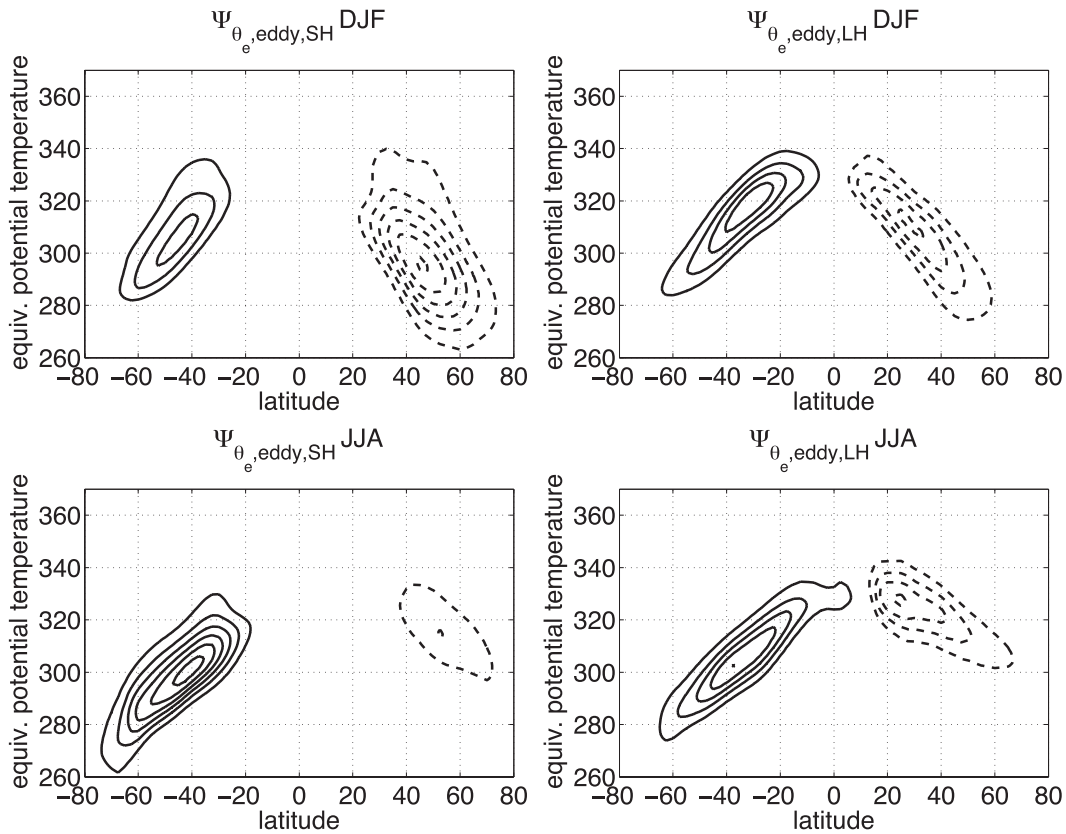


FIG. 5. The (left) sensible and (right) latent heat flux contributions to the STEM eddy circulation on moist isentropes during (top) DJF and (bottom) JJA. Contouring is as in Fig. 1.

a shallow surface layer corresponding to a strong return flow in a narrow range of isentropic surfaces. This thickness is proportional to the eddy variance and thus the return flow at the surface becomes infinite in the small variance limit as it does in the TEM formulation.

### 5. Effective stratification

The relationship between the eddy variance and the mass transport in the STEM formulation can be further explored using the effective stratification, which is defined as

$$\Delta\zeta = \frac{|F_\zeta|}{\Delta\Psi_\zeta}, \quad (17)$$

where  $\Delta\Psi_\zeta$  is the total mass transport in  $\zeta$  coordinates [(13)] and

$$F_\zeta = \int_{-\infty}^{\infty} \tilde{\zeta} M_\zeta d\tilde{\zeta} = \int_0^{\infty} 2\pi a \cos\phi (\bar{v}\tilde{\zeta} + \overline{v'\zeta'}) \frac{d\tilde{p}}{g} \quad (18)$$

is the meridional  $\zeta$  transport. Qualitatively, the effective stratification can be interpreted as the thickness of the

overturning cell in  $\zeta$  coordinates. The STEM formulation preserves the meridional  $\zeta$  transport. In Fig. 7 it is clear that changes in the  $\theta$  thickness of the circulation (i.e., the effective stratification  $\Delta\theta$ ) is compensated for by a change in the total mass transport so as to maintain a constant meridional  $\theta$  transport. In particular, as the constant eddy variance is decreased, the effective stratification decreases and the mass transport increases so as to keep the meridional  $\theta$  transport constant. Overall, the dry and moist effective stratifications from the STEM formulation agree well with the exact calculations (not shown) and with the results of Pauluis et al. (2010), who also calculated the effective stratification using NCEP data (see their Fig. 7). The small errors in the STEM effective stratification are caused by errors in the total mass transport, which are up to 10% for the dry isentropic circulation and up to 5% for the moist isentropic circulation (see Fig. 6).

The largest differences between the dry and moist STEM circulations were the result of differences in the eddy-induced circulations, which dominate in midlatitudes. In particular, the eddy-induced circulation was much stronger on moist isentropes and was related to

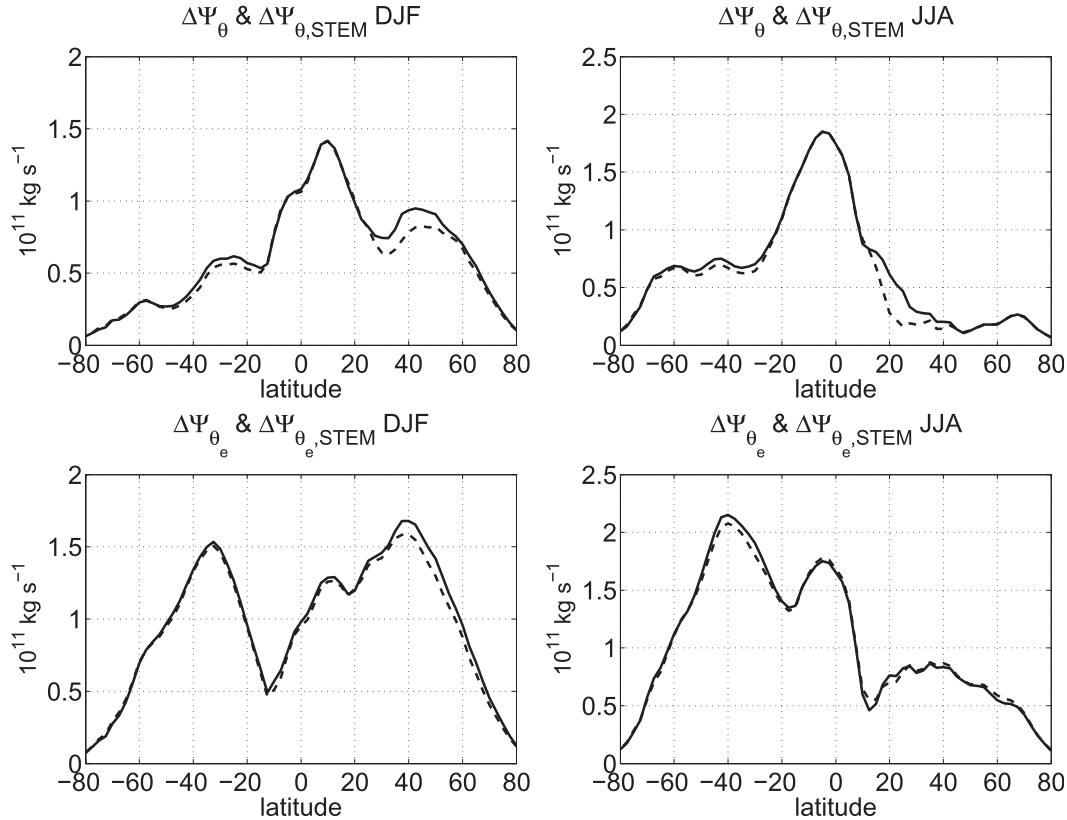


FIG. 6. The total isentropic mass transport during (left) DJF and (right) JJA on (top) dry and (bottom) moist isentropes for the exact circulation (solid line) and the STEM residual circulation (dashed line).

the latent heat transport (compare Figs. 1 and 2 to Figs. 3 and 4). The difference in strength between the dry and moist STEM eddy components lead to differences in the effective stratifications according to (22). The relative contributions of  $\overline{v'\zeta'}$  and  $\zeta'^2$  to the structure of the eddy-induced circulation and the effective stratification can be understood by considering an idealized atmosphere with constant eddy variance and poleward transport in a layer of thickness  $\Delta P$  and zero eddy variance and poleward transport elsewhere. We will also assume that the stratification  $\partial\bar{\zeta}/\partial p$  is constant and define the thickness of the layer in  $\zeta$  coordinates as  $\Delta Z = |\partial\bar{\zeta}/\partial p|\Delta P$ . Under these approximations, the eddy transport is

$$F_\zeta = \frac{2\pi a \cos\phi}{g} \Delta P \overline{v'\zeta'}. \quad (19)$$

It is shown in appendix C that the eddy mass transport is given by (C3):

$$\Delta\Psi_\zeta = \frac{2\pi a \cos\phi}{g} \left| \frac{\partial\bar{\zeta}}{\partial p} \right|^{-1} |\overline{v'\zeta'}| \operatorname{erf}\left(\frac{\sqrt{2}}{4}\Delta P^*\right), \quad (20)$$

where  $\operatorname{erf}$  is the error function and  $\Delta P^* = \Delta Z/\overline{\zeta'^2}^{1/2}$  is the ratio of the thickness of the layer in  $\zeta$  coordinates to the eddy variance  $\overline{\zeta'^2}^{1/2}$ . The effective stratification is then equal to

$$\Delta\zeta = \Delta Z \left[ \operatorname{erf}\left(\frac{\sqrt{2}}{4}\Delta P^*\right) \right]^{-1} = \Delta P^* \overline{\zeta'^2}^{1/2} \left[ \operatorname{erf}\left(\frac{\sqrt{2}}{4}\Delta P^*\right) \right]^{-1} \quad (21)$$

and depends on both the vertical variation of  $\zeta$  (through  $\Delta Z$ ) and the eddy variance (through  $\Delta P^*$ ).

To better understand the dependence of the effective stratification (21) on  $\Delta P^*$  we consider two limiting cases. If the relative thickness is large (i.e., if the vertical variation of  $\zeta$  through the layer is large compared to the eddy variance), then

$$\lim_{\Delta P^* \rightarrow \infty} \Delta\Psi_\zeta = \frac{2\pi a \cos\phi}{g} \left| \frac{\partial\bar{\zeta}}{\partial p} \right|^{-1} |\overline{v'\zeta'}|, \quad (22)$$

which equals the eddy mass transport in the TEM formulation. The corresponding effective stratification is

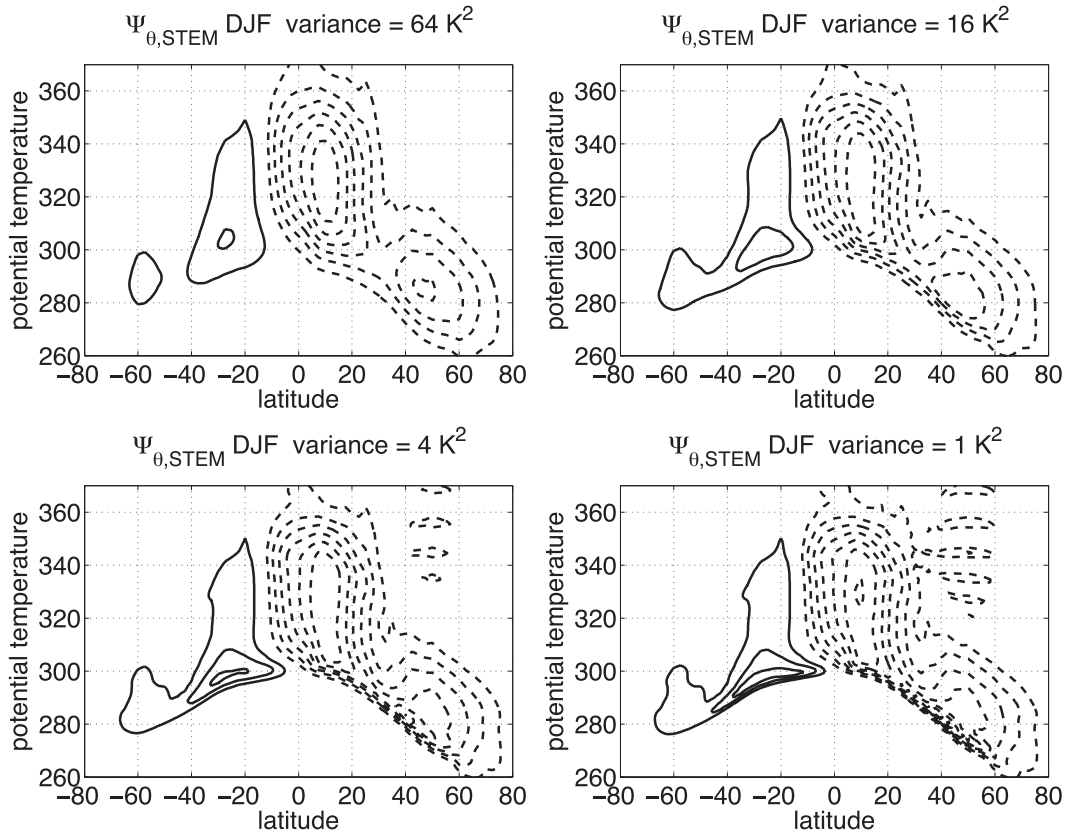


FIG. 7. The STEM residual circulation on dry isentropes during DJF for  $\overline{\theta'^2} = \text{constant}$  [ $\overline{\theta'^2} =$  (top left)  $64 \text{ K}^2$ , (top right)  $16 \text{ K}^2$ , (bottom left)  $4 \text{ K}^2$ , and (bottom right)  $1 \text{ K}^2$ ]. Contouring is as in Fig. 1.

$$\lim_{\Delta P^* \rightarrow \infty} \Delta \zeta = \Delta Z. \quad (23)$$

If the relative thickness is small (i.e., if the vertical variation of  $\zeta$  through the layer is small), the effective stratification is obtained by taking the limit of (21) for small  $\Delta P^*$ :

$$\begin{aligned} \lim_{\Delta P^* \rightarrow 0} \Delta \zeta &= \lim_{\Delta P^* \rightarrow 0} \frac{\overline{\zeta'^2}^{1/2}}{\zeta'^2} \frac{\Delta P^*}{\text{erf}\left(\frac{\sqrt{2}}{4} \Delta P^*\right)} \\ &= \frac{\overline{\zeta'^2}^{1/2}}{\frac{d}{dx} \text{erf}\left(\frac{\sqrt{2}}{4} x\right)_{x=0}} = \sqrt{2\pi} \overline{\zeta'^2}^{1/2} \approx 2.5 \overline{\zeta'^2}^{1/2}. \end{aligned} \quad (24)$$

Note that the constant prefactor is a result of the Gaussian distribution assumption.

We can use this simple model of the effective stratification to understand the effective stratifications associated with the dry and moist isentropic circulations (i.e.,  $\Delta\theta$  and  $\Delta\theta_e$ ). Figure 8 shows the eddy meridional transport (top), the temporal and zonal-mean (middle),

and the eddy variance (lower) of the potential temperature (left) and equivalent potential temperature (right) from  $10^\circ$  to  $70^\circ\text{N}$  during JJA. The meridional eddy potential temperature flux spans the entire troposphere poleward of the storm track (roughly north of  $40^\circ\text{N}$ ). The vertical variation of potential temperature from the surface to 500 hPa at  $40^\circ\text{N}$  is  $\Delta p \partial \bar{\theta} / \partial p \sim 25 \text{ K}$ , which is significantly larger than the eddy standard deviation  $\overline{\theta'^2}^{1/2} \sim 6 \text{ K}$ . Thus,  $\Delta\theta$  can be approximated by the large thickness limit (23):

$$\Delta\theta \approx \frac{\partial \bar{\theta}}{\partial p} \Delta p. \quad (25)$$

In contrast, on the equatorward side of the storm track (roughly between  $15^\circ$  and  $40^\circ\text{N}$ ), the eddy transport of equivalent potential temperature is confined to a shallow layer near the surface. The transport is dominated by latent heat transport.<sup>1</sup> The vertical variation of equivalent

<sup>1</sup> Poleward of  $45^\circ$  the transport of equivalent potential temperature is a mixture of latent and sensible heat and does not satisfy the approximation of uniform eddy statistics discussed above.

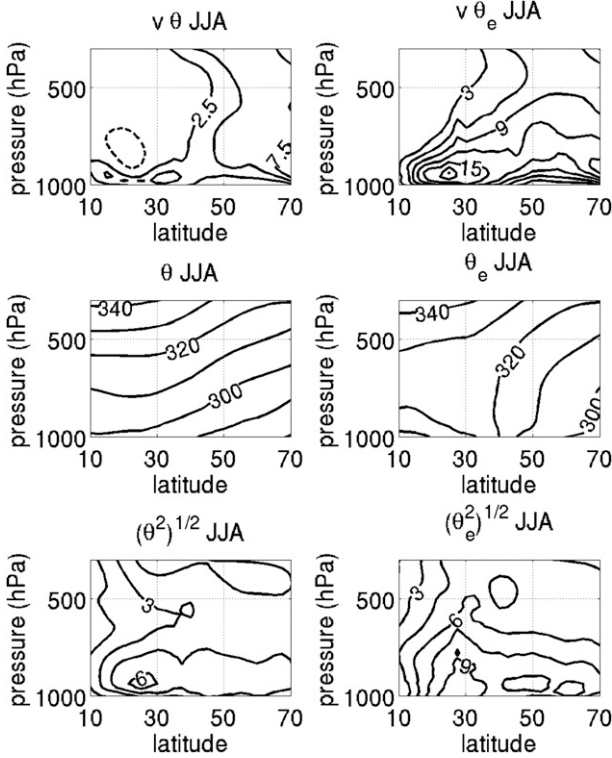


FIG. 8. (top) Eddy meridional transport, (middle) mean value, and (bottom) eddy standard deviation of (left)  $\theta$  and (right)  $\theta_e$  during JJA. Contour intervals are (top)  $2.5 \text{ km}^{-1}$ , (middle)  $10 \text{ K}$ , and (bottom)  $1.5 \text{ K}$ , with dashed contours representing negative values.

potential temperature from the surface to 500 hPa is near zero in the Northern Hemisphere subtropics, whereas the eddy standard deviation  $\overline{\theta'^2}^{1/2} \sim 9\text{K}$ . Thus, the effective stratification for  $\theta_e$  in the subtropics can be approximated by the small thickness limit (24):

$$\Delta\theta_e \approx 2.5\overline{\theta'^2_e}^{1/2}. \tag{26}$$

Pauluis et al. (2010) found that the dry and moist effective stratifications are approximately equal across the storm tracks:

$$\Delta\theta \approx \Delta\theta_e.$$

According to the two approximations (25) and (26), this implies that in midlatitudes

$$\frac{\partial\bar{\theta}}{\partial p} \Delta p \approx 2.5\overline{\theta'^2_e}^{1/2}. \tag{27}$$

Therefore, the vertical increase in potential temperature is directly tied to the eddy-induced fluctuations of equivalent potential temperature in the lower troposphere.

This result is in agreement with Juckes (2000) and Frierson (2006, 2008), who argue that the midlatitude stratification is set by moist convection in baroclinic eddies. While the derivation of (27) here is based on kinematic arguments and the comparison between the dry and moist isentropic circulations, it also emphasizes the role of moist ascent in the midlatitude storm tracks.

Interestingly, the small relative thickness limit (27) suggests that the dry stratification should be larger than the standard deviation of  $\theta_e$  by a factor of approximately 2.5.<sup>2</sup> In the STEM formulation, the mean value of the equivalent potential temperature in the poleward component of the flow is given by

$$\theta_e^+ \approx \bar{\theta}_e + 1.25\overline{\theta'^2_e}^{1/2}. \tag{28}$$

This value corresponds to the 89th percentile of the cumulative Gaussian distribution. While  $\theta_e^+$  is a typical value of  $\theta_e$  for poleward-moving air parcels, it corresponds to a relatively large and rare fluctuation of  $\theta_e$  at the same latitude. This is a consequence of the fact that if there is a poleward eddy transport of equivalent potential temperature, the meridional velocity and  $\theta_e$  are correlated and the distribution of  $\theta_e$  for poleward-moving air parcels is displaced toward higher value of  $\theta_e$ . In particular, if the midlatitude stratification is indeed determined by the equivalent potential temperature of poleward-moving air parcels, then the implication is that the large majority of air parcels at that latitude would still experience a stable stratification for moist displacement.

### 6. Summary and discussion

In this paper we have derived a statistical generalization of the transformed Eulerian-mean circulation. The formulation is based on a Gaussian assumption for the joint distribution of  $v$  and a state variable  $\zeta$ , which makes it possible to compute the meridional mass transport on iso- $\zeta$  surfaces. The corresponding streamfunction is computed by integrating the mass transport. As for the TEM residual circulation, the STEM residual circulation can be decomposed into Eulerian-mean and eddy components. The Eulerian-mean component of the circulation involves the convolution of the time- and zonally averaged mean meridional velocity with a Gaussian distribution whose structure is determined by the eddy variance of  $\zeta$ , while the eddy component involves the

<sup>2</sup> The exact factor depends on the Gaussian approximation and would change for a different distribution.

convolution of the time- and zonally averaged meridional eddy transport with the derivative of the Gaussian distribution. Unlike the TEM formulation, the STEM formulation does not require that  $\zeta$  be stratified in the vertical. The STEM formulation can therefore be applied to variables  $\zeta$  that are not monotonic such as the equivalent potential temperature.

The STEM residual circulation was computed for DJF and JJA using monthly and zonally averaged NCEP data for  $\zeta = \theta$  and  $\zeta = \theta_e$ . The dry and moist STEM residual circulations were found to be in very good agreement with exact calculations of the isentropic circulations. The STEM residual circulations capture all of the qualitative features of the isentropic circulations. The error in the mass transport is less than 10% even for the moist isentropic circulation.

The STEM formulation was subsequently used to assess the relative roles of eddy sensible and latent heat transport in the moist circulation. The eddy sensible heat transport dominates in the midlatitudes, while the eddy latent heat transport dominates in the subtropical regions. The latent heat transport contribution accounts for moisture transport by baroclinic eddies, which extract water vapor from the subtropics and deposit it in the extratropics. The transport is associated with a poleward flow of air at high  $\theta_e$  that is balanced by an equatorward flow of air with low  $\theta_e$ . During both DJF and JJA the sensible heat transport dominates in the winter hemisphere while the latent transport dominates in the summer hemisphere. This is in contrast to the dry isentropic circulation where the STEM eddy circulation in the summer hemisphere during JJA is very weak.

The effective stratification introduced in Pauluis et al. (2010) can be approximated under the STEM formulation and is shown to involve both the vertical stratification and the eddy variance. For the dry isentropic circulation, the approximate effective stratification is dominated by the vertical stratification, whereas for the moist isentropic circulation it is dominated by the eddy variance contribution. The approximate effective stratification suggests that the midlatitude potential temperature vertical lapse rate is tied directly to the eddy-induced fluctuations of equivalent potential temperature (i.e., the eddy variance) in the lower troposphere. This approximate relationship between the lapse rate and the eddy variance in the midlatitudes is consistent with Jukes (2001), who suggested that in the midlatitudes, the potential temperature stratification is tied to horizontal fluctuation of the equivalent potential temperature.

The STEM formulation can be viewed as a generalization of the TEM formulation. It was shown that if  $\bar{\zeta}$  is stratified in the vertical, then the TEM circulation can be obtained from the STEM formulation in the limit

of small eddy variance. The STEM offers two key advantages over the TEM. First, it does not require that the new coordinate  $\zeta$  be monotonic in the vertical and can thus be applied for a wide range of variables such as the equivalent potential temperature, which exhibits a local extremum in the vertical. Second, it accounts for the magnitude of fluctuations of the variable  $\zeta$ . In doing so, STEM avoids the problem of the infinite return flow at the earth's surface that often occurs in the TEM formulation.

It is natural to wonder how it is possible to apply the STEM formulation to nonmonotonic coordinates when the TEM formulation fails to apply. First, the STEM formulation transforms the mean meridional circulation to a new coordinate  $\zeta$  instead of keeping the vertical pressure coordinate. For a nonmonotonic state variable  $\bar{\zeta}$ , the transformation  $p \rightarrow \zeta = \bar{\zeta}(p)$  is well defined but its inverse  $\zeta \rightarrow p$  is not. By deliberately computing the streamfunction in terms of  $\zeta$  and not  $p$  one avoids having to perform an unsolvable inversion. This of course comes with the caveat that the circulation involves a nonmonotonic vertical coordinate and hence cannot be everywhere interpreted as a vertical overturning flow. Second, the TEM formulation, and in particular its interpretation in terms of the generalized Lagrangian mean formulation (Andrews and McIntyre 1978; McIntyre 1980), associates eddy fluctuations with vertical displacement and replaces eddy transport by a vertical overturning. This formulation breaks down near a local minimum or maximum for  $\bar{\zeta}$  where small displacements cannot produce the required fluctuations. As discussed by Plumb and Ferrari (2005), the TEM formulation cannot account for eddy transport in the direction orthogonal to the mean iso- $\zeta$  surfaces. In contrast, the STEM directly accounts for the eddy fluctuations at a given pressure level because it takes into account the eddy variance. In effect, an extra dimension  $\zeta$  is added before averaging out the Eulerian coordinate. This makes it possible to perform the coordinate transformation even when the eddy fluctuations cannot be re-expressed in terms of the old vertical coordinates by removing the direct link between eddy fluctuations and displacement.

Several issues remain open for future investigation. First, the STEM formulation proposed here is purely kinematic. Its derivation does not require any dynamical information besides the eddy statistics. Connecting the STEM residual circulation to the well-known Eliassen-Palm (EP) flux is the subject of current research. More generally, this requires gaining a better understanding on the relationship between the isentropic mass transport and the momentum transport. Second, the assumption that the eddy statistics obey a Gaussian distribution

needs to be further evaluated. While this assumption has been shown here to capture most of the qualitative and quantitative features of the isentropic circulations, the formulation could be extended to accounting for higher-order moment and different distributions. Different distributions may be required for different applications such as the oceanic circulation. They may also provide new insight into the contribution of extreme events, which fall outside a Gaussian distribution, to the global circulation.

The STEM approach offers a computationally efficient and accurate method to obtain the global atmospheric circulation on either dry or moist isentropes. As such, the STEM circulations from different general circulation models can be compared and used to identify important differences between the modeled midlatitude baroclinic eddies. Furthermore, systematic studies of the global atmospheric circulation in isentropic coordinates, such as that of Laliberté and Pauluis (2010), who analyzed simulations from the Intergovernmental Panel on Climate Change Fourth Assessment Report (IPCC AR4) model archive to quantify the effects of climate change on the isentropic circulations, can provide new insights into the variability of the earth’s climate. In this context, implementing STEM as a standard diagnostic for climate models should make it possible to both improve the ability of these models to capture the dynamics of the storm tracks and to further assess the variability of the global atmospheric circulation.

*Acknowledgments.* We thank NCEP for providing the reanalysis data set. This work was supported by the NSF under Grant AGS-0944058. Tiffany Shaw acknowledges

support from the Natural Sciences and Engineering Research Council of Canada through a postdoctoral fellowship.

## APPENDIX A

### Meridional Mass Transport Associated with a Gaussian Distribution

Given the joint probability density function  $f(v, \zeta)$  for the meridional wind  $v$  and the state variable  $\zeta$  at a fixed pressure  $p$  and latitude  $\phi$ , the associated joint distribution for the meridional mass transport per unit  $\zeta$  and unit  $p$  is

$$m(p, \zeta, \phi) = \frac{2\pi a \cos\phi}{g} \int_{-\infty}^{\infty} v f(v, \zeta) dv. \quad (A1)$$

If the probability density function is a bivariate Gaussian distribution—that is,

$$f(v, \zeta) = \frac{1}{2\pi|\Sigma|^{1/2}} \exp\left[-\frac{1}{2}(\mathbf{v}', \zeta')^T \Sigma^{-1}(\mathbf{v}', \zeta')\right], \quad (A2)$$

where  $\mathbf{v}' = v - \bar{v}$  and  $\zeta' = \zeta - \bar{\zeta}$  are the departures from the mean values  $\bar{v}$  and  $\bar{\zeta}$  and  $\Sigma$  is the covariance matrix,

$$\Sigma = \begin{vmatrix} \overline{v'^2} & \overline{v'\zeta'} \\ \overline{v'\zeta'} & \overline{\zeta'^2} \end{vmatrix} \quad (A3)$$

—then the probability density function can be rewritten as the product of two Gaussian distributions:

$$\begin{aligned} f(v, \zeta) &= \frac{1}{2\pi|\Sigma|^{1/2}} \exp\left(-\frac{\overline{\zeta'^2}v'^2 - 2\overline{v'\zeta'}v'\zeta' + \overline{v'^2}\zeta'^2}{2|\Sigma|}\right) \\ &= \frac{\overline{\zeta'^2}^{1/2}}{\sqrt{2\pi|\Sigma|^{1/2}}} \exp\left[\frac{-\zeta'^2}{2|\Sigma|}\left(v' - \frac{\overline{v'\zeta'}}{\overline{\zeta'^2}}\zeta'\right)^2\right] \frac{1}{\sqrt{2\pi\overline{\zeta'^2}^{1/2}}} \exp\left(\frac{-\zeta'^2}{2\overline{\zeta'^2}}\right) \\ &= \mathcal{N}\left(\bar{v} + \frac{\overline{v'\zeta'}}{\overline{\zeta'^2}}\zeta', \frac{|\Sigma|}{\overline{\zeta'^2}}\right) \mathcal{N}(\bar{\zeta}, \overline{\zeta'^2}), \end{aligned} \quad (A4)$$

where  $\mathcal{N}(\mu, \sigma^2)$  denotes a Gaussian distribution with mean  $\mu$  and variance  $\sigma^2$ . The first Gaussian distribution on the right-hand side of (A4) corresponds to the conditional probability density of  $v$  for a given value of  $\zeta$ . The second Gaussian on the right-hand side of (A4)

can be viewed as the probability density function for  $\zeta$  alone.

The joint distribution of meridional mass transport per unit  $\zeta$  and unit  $p$  can be obtained by substituting (A4) into (A1); for example,

$$\begin{aligned}
 m(p, \zeta, \phi) &= \frac{2\pi a \cos\phi}{g} \left[ \int_{-\infty}^{\infty} v \mathcal{N} \left( \bar{v} + \frac{\bar{v}'\zeta'}{\zeta'^2} \zeta', \frac{|\Sigma|}{\zeta'^{2/2}} \right) dv \right] \mathcal{N}(\bar{\zeta}, \bar{\zeta}'^{1/2}) \\
 &= \frac{2\pi a \cos\phi}{g} \frac{1}{\sqrt{2\pi\bar{\zeta}'^{1/2}}} \left[ \bar{v} + \frac{\bar{v}'\zeta'}{\zeta'^2} (\zeta - \bar{\zeta}) \right] \exp \left[ -\frac{(\zeta - \bar{\zeta})^2}{2\bar{\zeta}'^{1/2}} \right], \tag{A5}
 \end{aligned}$$

which can be easily decomposed into Eulerian-mean and eddy components:

$$m_{\text{mean}}(p, \zeta, \phi) = \frac{2\pi a \cos\phi}{g} \frac{\bar{v}}{\sqrt{2\pi\bar{\zeta}'^{1/2}}} \exp \left[ -\frac{(\zeta - \bar{\zeta})^2}{2\bar{\zeta}'^{1/2}} \right], \tag{A6a}$$

$$m_{\text{eddy}}(p, \zeta, \phi) = \frac{2\pi a \cos\phi}{g} \frac{\bar{v}'\zeta'(\zeta - \bar{\zeta})}{\sqrt{2\pi\bar{\zeta}'^{3/2}}} \exp \left[ -\frac{(\zeta - \bar{\zeta})^2}{2\bar{\zeta}'^{1/2}} \right]. \tag{A6b}$$

APPENDIX B

The Small Variance Limit of the STEM Formulation

Here we show that the STEM circulation converges to the TEM circulation in the limit of small eddy variance. We begin by assuming that the mean vertical profile  $\bar{\zeta}(p)$  is monotonic, which ensures that the TEM circulation is well defined at all levels. It also implies that  $\bar{\zeta}(p)$  has a unique inverse  $p = \bar{\zeta}^{-1}(\zeta)$ . We consider the STEM circulation for a constant eddy variance  $\zeta'^2$  and consider the limit of the eddy variance going to zero (i.e., for  $\lim \zeta'^2 \rightarrow 0$ ). Under these assumptions, the Eulerian-mean component of the STEM streamfunction (9a) becomes

$$\begin{aligned}
 \lim_{\zeta'^2 \rightarrow 0} \Psi_{\zeta, \text{mean}}(\zeta, \phi) &= \lim_{\zeta'^2 \rightarrow 0} \int_{-\infty}^{\zeta} \int_0^{\infty} \frac{2\pi a \cos\phi}{g} \frac{\bar{v}}{\sqrt{2\pi\bar{\zeta}'^{1/2}}} \exp \left[ -\frac{(\tilde{\zeta} - \bar{\zeta})^2}{2\bar{\zeta}'^{1/2}} \right] d\tilde{p} d\tilde{\zeta} \\
 &= \int_0^{\infty} \frac{2\pi a \cos\phi}{g} \bar{v} \left\{ \lim_{\zeta'^2 \rightarrow 0} \int_{-\infty}^{\zeta} \frac{1}{\sqrt{2\pi\bar{\zeta}'^{1/2}}} \exp \left[ -\frac{(\tilde{\zeta} - \bar{\zeta})^2}{2\bar{\zeta}'^{1/2}} \right] d\tilde{\zeta} \right\} d\tilde{p} \tag{B1}
 \end{aligned}$$

after changing the order of integration and moving the limit inside the integral. The small variance limit of the inner integral is

$$\begin{aligned}
 &\lim_{\zeta'^2 \rightarrow 0} \int_{-\infty}^{\zeta} \frac{1}{\sqrt{2\pi\bar{\zeta}'^{1/2}}} \exp \left[ -\frac{(\tilde{\zeta} - \bar{\zeta})^2}{2\bar{\zeta}'^{1/2}} \right] d\tilde{\zeta} \\
 &= \begin{cases} 1 & \text{if } \tilde{\zeta} > \bar{\zeta} \\ \frac{1}{2} & \text{if } \tilde{\zeta} = \bar{\zeta}. \\ 0 & \text{otherwise} \end{cases} \tag{B2}
 \end{aligned}$$

If the function  $\bar{\zeta}(p)$  increases monotonically then this limit converges (in the weak sense) to the Heaviside step function  $H(p - \bar{p})$  and hence (B1) becomes

$$\begin{aligned}
 \lim_{\zeta'^2 \rightarrow 0} \Psi_{\zeta, \text{mean}}(\zeta, \phi) &= \int_0^{\infty} \frac{2\pi a \cos\phi}{g} \bar{v} H(p - \bar{p}) d\bar{p} \\
 &= \int_0^p \frac{2\pi a \cos\phi}{g} \bar{v} d\bar{p} = \Psi_{p, \text{mean}}(p, \phi), \tag{B3}
 \end{aligned}$$

where  $\Psi_{p, \text{mean}}$  is the mean meridional circulation averaged in pressure coordinates, which is evaluated at the pressure  $p$  such that  $\bar{\zeta}(p) = \zeta$ . If  $\bar{\zeta}(p)$  decreases monotonically, then the limit (B2) is equal to the Heaviside step function  $H(\bar{p} - p)$  and the integral (B1) is equal to  $-\Psi_{p, \text{mean}}(p, \phi)$ .

The small variance limit can also be applied to the eddy component of the STEM circulation (9b) to obtain

$$\lim_{\zeta'^2 \rightarrow 0} \Psi_{\zeta, \text{eddy}}(\zeta, \phi) = \lim_{\zeta'^2 \rightarrow 0} \int_{-\infty}^{\zeta} \int_0^{\infty} \frac{2\pi a \cos\phi}{g} \frac{\bar{v}'\zeta'}{\sqrt{2\pi\bar{\zeta}'^{3/2}}} (\tilde{\zeta} - \bar{\zeta}) \exp \left[ -\frac{(\tilde{\zeta} - \bar{\zeta})^2}{2\bar{\zeta}'^{1/2}} \right] d\tilde{p} d\tilde{\zeta}. \tag{B4}$$

After integration by parts, the inner integral becomes

$$\begin{aligned} \int_0^\infty \frac{\overline{v'\zeta'}}{\sqrt{2\pi\zeta'^2}^{3/2}}(\zeta - \bar{\zeta}) \exp\left[-\frac{(\zeta - \bar{\zeta})^2}{2\zeta'^2}\right] d\bar{p} &= \int_0^\infty \left(\frac{d\bar{\zeta}}{d\bar{p}}\right)^{-1} \overline{v'\zeta'} \left\{ \frac{d\bar{\zeta}}{d\bar{p}} \frac{(\zeta - \bar{\zeta})}{\sqrt{2\pi\zeta'^2}^{3/2}} \exp\left[-\frac{(\zeta - \bar{\zeta})^2}{2\zeta'^2}\right] \right\} d\bar{p} \\ &= \left\{ \frac{1}{g} \left(\frac{d\bar{\zeta}}{d\bar{p}}\right)^{-1} \overline{v'\zeta'} \frac{1}{\sqrt{2\pi\zeta'^2}^{1/2}} \exp\left[-\frac{(\zeta - \bar{\zeta})^2}{2\zeta'^2}\right] \right\}_{\bar{p}=0}^{\bar{p}=\infty} \\ &\quad - \int_0^\infty \frac{d}{d\bar{p}} \left[ \left(\frac{d\bar{\zeta}}{d\bar{p}}\right)^{-1} \overline{v'\zeta'} \right] \frac{1}{\sqrt{2\pi\zeta'^2}^{1/2}} \exp\left[-\frac{(\zeta - \bar{\zeta})^2}{2\zeta'^2}\right] d\bar{p}. \end{aligned} \tag{B5}$$

Upon inserting (B5) into (B4), we obtain

$$\begin{aligned} \lim_{\zeta'^2 \rightarrow 0} \Psi_{\zeta,\text{eddy}}(\zeta, \phi) &= - \left[ \frac{2\pi a \cos\phi}{g} \left(\frac{d\bar{\zeta}}{d\bar{p}}\right)^{-1} \overline{v'\zeta'}(0) \right] \left\langle \lim_{\zeta'^2 \rightarrow 0} \int_{-\infty}^{\zeta} \frac{1}{\sqrt{2\pi\zeta'^2}^{1/2}} \exp\left\{-\frac{[\zeta - \bar{\zeta}(0)]^2}{2\zeta'^2}\right\} d\bar{\zeta} \right\rangle \\ &\quad + \left[ \frac{2\pi a \cos\phi}{g} \left(\frac{d\bar{\zeta}}{d\bar{p}}\right)^{-1} \overline{v'\zeta'}(\infty) \right] \left\langle \lim_{\zeta'^2 \rightarrow 0} \int_{-\infty}^{\zeta} \frac{1}{\sqrt{2\pi\zeta'^2}^{1/2}} \exp\left\{-\frac{[\zeta - \bar{\zeta}(\infty)]^2}{2\zeta'^2}\right\} d\bar{\zeta} \right\rangle \\ &\quad - \int_0^\infty \frac{2\pi a \cos\phi}{g} \frac{d}{d\bar{p}} \left[ \left(\frac{d\bar{\zeta}}{d\bar{p}}\right)^{-1} \overline{v'\zeta'} \right] \left\{ \lim_{\zeta'^2 \rightarrow 0} \int_{-\infty}^{\zeta} \frac{1}{\sqrt{2\pi\zeta'^2}^{1/2}} \exp\left[-\frac{(\zeta - \bar{\zeta})^2}{2\zeta'^2}\right] d\bar{\zeta} \right\} d\bar{p}. \end{aligned} \tag{B6}$$

Upon replacing the limit by (B2) we obtain, for a uniformly increasing  $\bar{\zeta}(p)$ ,

$$\begin{aligned} \lim_{\zeta'^2 \rightarrow 0} \Psi_{\zeta,\text{eddy}}(\zeta, \phi) &= - \frac{2\pi a \cos\phi}{g} \left(\frac{d\bar{\zeta}}{dp}\right)^{-1} \overline{v'\zeta'}(0) \\ &\quad - \int_0^p \frac{2\pi a \cos\phi}{g} \frac{d}{d\bar{p}} \left[ \left(\frac{d\bar{\zeta}}{d\bar{p}}\right)^{-1} \overline{v'\zeta'} \right] d\bar{p} \\ &= - \frac{2\pi a \cos\phi}{g} \left(\frac{d\bar{\zeta}}{dp}\right)^{-1} \overline{v'\zeta'}(p) = \Psi_{p,\text{eddy}} \end{aligned} \tag{B7}$$

and, for a decreasing  $\bar{\zeta}(p)$ ,

$$\begin{aligned} \lim_{\zeta'^2 \rightarrow 0} \Psi_{\zeta,\text{eddy}}(\zeta, \phi) &= \frac{2\pi a \cos\phi}{g} \left(\frac{d\bar{\zeta}}{dp}\right)^{-1} \overline{v'\zeta'}(\infty) \\ &\quad - \int_p^\infty \frac{2\pi a \cos\phi}{g} \frac{d}{d\bar{p}} \left[ \left(\frac{d\bar{\zeta}}{d\bar{p}}\right)^{-1} \overline{v'\zeta'} \right] d\bar{p} \\ &= - \frac{2\pi a \cos\phi}{g} \left(\frac{d\bar{\zeta}}{dp}\right)^{-1} \overline{v'\zeta'}(p) = -\Psi_{p,\text{eddy}}, \end{aligned} \tag{B8}$$

where  $\Psi_{p,\text{eddy}}$  is exactly the eddy component of the TEM circulation.

### APPENDIX C

#### Total Mass Transport and Effective Stratification for an Idealized Atmosphere

Consider an idealized atmosphere with a constant eddy variance  $\overline{\zeta'^2}$  and eddy transport  $\overline{v'\zeta'}$  between  $p = p_0 - \Delta P$  and  $p = p_0$  and zero elsewhere, with a constant mean stratification  $\partial\bar{\zeta}/\partial p$ . The layer thickness measured in  $\zeta$  coordinates is given by  $\Delta Z = |\partial\bar{\zeta}/\partial p| \Delta P$ . The corresponding eddy  $\zeta$  transport in this region is given by

$$F_\zeta = \int_{p_0 - \Delta P}^{p_0} \frac{2\pi a \cos\phi}{g} \overline{v'\zeta'} d\bar{p} = \frac{2\pi a \cos\phi}{g} \overline{v'\zeta'} \Delta P. \tag{C1}$$

The eddy contribution to the STEM circulation is given by (9b) and because of the symmetry of the integral it maximizes in the middle of the layer where  $\zeta_m = \bar{\zeta}(p_0 - \Delta P/2)$ ; that is,



$$\begin{aligned}
\Psi_{\zeta, \text{eddy}}(\zeta_m) &= \int_{p_0 - \Delta P}^{p_0} \int_{-\infty}^{\zeta_m} \frac{2\pi a \cos\phi}{g} \frac{\overline{v'\zeta'}}{\sqrt{2\pi\zeta'^2}^{3/2}} [\tilde{\zeta} - \bar{\zeta}(\bar{p})] \exp\left\{-\frac{[\tilde{\zeta} - \bar{\zeta}(\bar{p})]^2}{2\zeta'^2}\right\} d\tilde{\zeta} d\bar{p} \\
&= \int_{-\Delta P/2}^{\Delta P/2} \int_{-\infty}^0 \frac{2\pi a \cos\phi}{g} \frac{\overline{v'\zeta'}}{\sqrt{2\pi\zeta'^2}^{3/2}} \left[\hat{\zeta} + \zeta_m - \bar{\zeta}\left(\frac{\Delta P}{2} + \hat{p}\right)\right] \exp\left\{-\frac{\left[\hat{\zeta} + \zeta_m - \bar{\zeta}\left(\frac{\Delta P}{2} + \hat{p}\right)\right]^2}{2\zeta'^2}\right\} d\hat{\zeta} d\hat{p} \\
&= \int_{-\Delta P/2}^{\Delta P/2} \int_{-\infty}^0 \frac{2\pi a \cos\phi}{g} \frac{\overline{v'\zeta'}}{\sqrt{2\pi\zeta'^2}^{3/2}} \left(\hat{\zeta} - \frac{\partial\bar{\zeta}}{\partial\hat{p}}\hat{p}\right) \exp\left[-\frac{\left(\hat{\zeta} - \frac{\partial\bar{\zeta}}{\partial\hat{p}}\hat{p}\right)^2}{2\zeta'^2}\right] d\hat{\zeta} d\hat{p} \\
&= - \int_{-\Delta P/2}^{\Delta P/2} \frac{2\pi a \cos\phi}{g} \frac{\overline{v'\zeta'}}{\sqrt{2\pi\zeta'^2}^{1/2}} \exp\left[-\frac{\left(\frac{\partial\bar{\zeta}}{\partial\hat{p}}\hat{p}\right)^2}{2\zeta'^2}\right] d\hat{p}, \tag{C2}
\end{aligned}$$

where the second and third lines are obtained after performing the change of variables  $\hat{p} = \bar{p} - (p_0 - \Delta P/2)$  and

$\hat{\zeta} = \tilde{\zeta} - \zeta_m$  and the last line is to be obtained through direct integration. Upon setting  $p^* = (\partial\bar{\zeta}/\partial p)\hat{p}/\zeta'^{1/2}$ , we obtain

$$\begin{aligned}
\Psi_{\zeta, \text{eddy}}(\zeta_m) &= -\frac{2\pi a \cos\phi}{g} \left|\frac{\partial\bar{\zeta}}{\partial p}\right|^{-1} \overline{v'\zeta'} \int_{-\Delta P^*/2}^{\Delta P^*/2} \frac{1}{\sqrt{2\pi}} \exp\left(-\frac{p^{*2}}{2}\right) dp^* \\
&= -\frac{2\pi a \cos\phi}{g} \left|\frac{\partial\bar{\zeta}}{\partial p}\right|^{-1} \overline{v'\zeta'} \int_0^{\Delta P^*/2} \sqrt{\frac{2}{\pi}} \exp\left(-\frac{p^{*2}}{2}\right) dp^* = -\frac{2\pi a \cos\phi}{g} \left|\frac{\partial\bar{\zeta}}{\partial p}\right|^{-1} \overline{v'\zeta'} \operatorname{erf}\left(\frac{\sqrt{2}\Delta P^*}{4}\right), \tag{C3}
\end{aligned}$$

where  $\Delta P^* = \Delta Z/\zeta'^{1/2}$ . Finally, the effective stratification (17) is

$$\Delta\zeta = \frac{F_\zeta}{\Psi_{\zeta, \text{eddy}}(\zeta_m)} = \Delta P \left|\frac{\partial\bar{\zeta}}{\partial p}\right| \left[\operatorname{erf}\left(\frac{\sqrt{2}\Delta P^*}{4}\right)\right]^{-1}. \tag{C4}$$

#### REFERENCES

- Andrews, D. G., and M. E. McIntyre, 1976: Planetary waves in horizontal and vertical shear: The generalized Eliassen–Palm relation and the zonal mean acceleration. *J. Atmos. Sci.*, **33**, 2031–2048.
- , and —, 1978: An exact theory of nonlinear waves on a Lagrangian-mean flow. *J. Fluid Mech.*, **89**, 609–646.
- , J. R. Holton, and C. B. Leovy, 1987: *Middle Atmosphere Dynamics*. 1st ed. Academic Press, 489 pp.
- Czaja, A., and J. Marshall, 2006: The partitioning of poleward heat transport between the atmosphere and ocean. *J. Atmos. Sci.*, **63**, 1498–1511.
- Döös, K., and J. Nilsson, 2011: Analysis of the meridional energy transport by atmospheric overturning circulations. *J. Atmos. Sci.*, **68**, 1806–1820.
- Edmon, H. J., B. J. Hoskins, and M. E. McIntyre, 1980: Eliassen–Palm cross sections for the troposphere. *J. Atmos. Sci.*, **37**, 2600–2616.
- Frierson, D. M. W., 2006: Robust increases in midlatitude static stability in global warming simulations. *Geophys. Res. Lett.*, **33**, L24816, doi:10.1029/2006GL027504.
- , 2008: Midlatitude static stability in simple and comprehensive general circulation models. *J. Atmos. Sci.*, **65**, 1049–1062.
- Held, I. M., and T. Schneider, 1999: The surface branch of the zonally averaged mass transport circulation in the troposphere. *J. Atmos. Sci.*, **56**, 1688–1697.
- Johnson, D. R., 1989: The forcing and maintenance of global monsoonal circulations: An isentropic analysis. *Adv. Geophys.*, **31**, 43–316.
- Jukes, M. N., 2000: The static stability of the midlatitude troposphere: The relevance of moisture. *J. Atmos. Sci.*, **57**, 3050–3057.
- , 2001: A generalization of the transformed Eulerian-mean meridional circulations. *Quart. J. Roy. Meteor. Soc.*, **127**, 147–160.
- , I. N. James, and M. Blackburn, 1994: The influence of Antarctica on the momentum budget of the southern extratropics. *Quart. J. Roy. Meteor. Soc.*, **120**, 1017–1044.
- Kalnay, E., and Coauthors, 1996: The NCEP/NCAR 40-Year Reanalysis Project. *Bull. Amer. Meteor. Soc.*, **77**, 437–471.
- Laliberté, F., and O. Pauluis, 2010: Winter intensification of the moist branch of the circulation in simulations of 21st century climate. *Geophys. Res. Lett.*, **37**, L20707, doi:10.1029/2010GL045007.
- McIntosh, P. C., and T. J. McDougall, 1996: Isopycnal averaging and the residual mean circulation. *J. Phys. Oceanogr.*, **26**, 1655–1660.

- McIntyre, M. E., 1980: An introduction to the generalized Lagrangian-mean description of wave, mean-flow interaction. *Pure Appl. Geophys.*, **118**, 152–176.
- Pauluis, O., A. Czaja, and R. Korty, 2008: The global atmospheric circulation on moist isentropes. *Science*, **321**, 1075–1078, doi:10.1126/science.1159649.
- , —, and —, 2010: The global atmospheric circulation in moist isentropic coordinates. *J. Climate*, **23**, 3077–3093.
- Peixoto, J. P., and A. H. Oort, 1992: *Physics of Climate*. AIP Press, 520 pp.
- Plumb, R. A., and R. Ferrari, 2005: Transformed Eulerian-mean theory. Part I: Nonquasigeostrophic theory for eddies on a zonal-mean flow. *J. Phys. Oceanogr.*, **35**, 165–174.
- Stone, P. H., and G. Salustri, 1984: Generalization of the quasigeostrophic Eliassen-Palm flux to include eddy forcing of condensation heating. *J. Atmos. Sci.*, **41**, 3527–3536.
- Townsend, R. D., and D. R. Johnson, 1985: A diagnostic study of the isentropic zonally averaged mass circulation during the first GARP global experiment. *J. Atmos. Sci.*, **42**, 1565–1579.